01 Jan 1971

Analysis of light gage steel shear diaphragms

Arthur H. Nilson

CCFSS LIBRARY Arthur H. Nilson ANALYSIS OF
22 3 * 21 LIGHT GAGE STEEL SHEAR
1971 DIAPHRAGMS

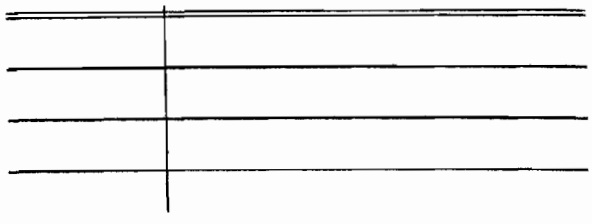

File: Joint Eng. Sub (Sheet) Project No. 1201-201

Analysis of Light Gage Steel Shear Diaphragms

by

Arthur H. Nilson*

Abstract

A method is presented for the elastic analysis of shear diaphragms composed of standard light gage steel panels. A finite element approach is adopted, in which the mechanical properties of the diaphragm components are incorporated in an analytical model of the assemblage, using the direct stiffness method of matrix structural analysis. Results are compared against experimental values.

*Professor and Acting Chairman, Dept. of Structural Engg., Cornell Univ., Ithaca, N.Y.

Introduction

Structural engineers have long been aware that light gage steel roof, floor, and wall panels of the types shown in Fig. 1 provide significant resistance to forces acting in the plane of their surface, in addition to resisting the normal loads for which they are usually designed (1,10). Countless designs have been executed over the past 20 years in which the shear diaphragm capacity of panel assemblies has been exploited.

Shear forces in the plane of the decking may come about in various situations. Fig. [illegible] a one-story building carrying lateral load from wind. The designer has at least three options. He can (a) design each frame with rigid joints to carry the horizontal forces, or (b) provide horizontal bracing just below the plane of the roof, or (c) make use of the decking as a shear-resisting membrane. The last choice is attractive because it uses the otherwise wasted shear capacity of the deck, it reduces or eliminates joint moments in the interior frames, and it avoids the need for unsightly bracing under the roof.

Vertical loads too may be resisted by shear membrane action. Fig. 3 shows a structure using rigid-jointed gable frames in conjunction with steel panel sheathing. A vertical load shown by the arrows at the top of the frames causes a tendency for the eaves to move outward. While the frames can be designed to accommodate this outward thrust, they will be needlessly heavy as a result. But note that the outward sway

the performance of specific combinations of panels, marginal framing members, purlins, and connections have been studied (6,8, 10,12). While much has been learned in this way, no rational theory has resulted. In addition, testing of large diaphragms is expensive and time consuming, and test results are applicable only to diaphragms using the same panels and fasteners as tested. The need for a general method of analysis is clear.

The research described in the present paper was directed toward the development of such a method of analysis. The approach taken was inspired by the finite element concept, developed in the aerospace industry and now finding many applications in the field of civil engineering structures. This approach provides the basis for the elastic analysis of shear diaphragms, to predict the effective shear modulus as well as the distribution of internal forces on all system components. Thus an alternative is provided to the AISI standard shear diaphragm test described in Ref. 1 and shown in Fig. 4.

Basis of Analysis

By the finite element method, problems in continuum mechanics, such as plane stress problems, can be solved using the same techniques that are commonly employed in the analysis of framed structures (13). The essential feature of the method is that an actual continuous body, such as a plate or a three-dimensional solid, is divided into a large number of small segments for purposes of analysis. Within each of these

regions, the strains may be defined in terms of relatively simple functions. The finite elements are assumed to be interconnected only at discrete points, called nodes, which are generally at the corners of the elements. By any of several means, the stiffness matrix relating the nodal forces to the nodal displacements of each element are found. The stiffness of the total assemblage is then found by superposition of the individual element stiffnesses, as by the ordinary methods of matrix analysis. After imposition of boundary conditions, the displacements of the nodes are found for any loading. The element strains are then obtained and the internal stresses easily found. The finite element idealization typically produces a highly redundant equivalent structure, with many nodes and many degrees of freedom. The resulting set of simultaneous joint equilibrium equations must be solved by computer.

An adaptation of the finite element method of analysis is particularly appropriate for shear diaphragms. These systems are, in actuality, composed of a large number of individual members, interconnected at discrete points, and a representation by some sort of a discretization is actually more realistic than one based on an equivalent continuum. Load is applied and reactions provided in the plane of the panels. The connections by which the forces are transferred are in the same plane. While marginal members and purlins generally have their centroid somewhat below the plane of the panels, tests have confirmed that the resulting eccentricity does not influence

the performance of shear diaphragms adversely. These members may be satisfactorily represented as being in the plane of the panels.

Thus a metal deck shear diaphragm can be idealized as a plane stress type problem in which each individual panel becomes, of itself, a finite element with nodes at points of interconnection with other panels or with marginal beams or purlins. The beams and purlins are represented as one-dimensional elements capable of resisting axial thrust as well as bending about vertical axes at their ends. Experience with actual diaphragms has shown that deformation at the connectors, particularly those along the seams between adjacent panels, plays an important part in determining the response of a diaphragm, and these are represented in the analysis by specially-devised spring-linkage elements permitting slight movements to occur between connected parts.

The basis for modelling the individual panels of a diaphragm depends on the type of panel. Simplest is the panel which has a flat sheet extending from one side of the panel to the other, stiffened by longitudinal ribs or by hat sections spot welded to the flat sheet (see Fig. 1). The relative stiffnesses are such that most of the membrane shears and thrusts are transmitted by the flat sheet, the other parts of the panel serving to stiffen that flat sheet. Such a panel is satisfactorily modelled as a uniform, isotropic elastic plate loaded in its own plane.

The open, corrugated type of panel is more complicated. Because of cross section geometry, extensional moduli in the two principal directions are much different, and the shear modulus is modified significantly as well. As a result, such panels must be represented as orthogonally anisotropic (orthotropic) elements.

In either case, nodes are established at the panel ends where they are attached to purlins or marginal beams, at panel edges where they are attached at intervals to adjacent panels, and (for exterior panels) along panel edges where they may be attached to marginal beams. Two degrees of freedom are established at each node, in the plane of the panel, parallel and perpendicular to the edges of the panel, as shown in Fig. 5. The panel stiffness can be found experimentally, analytically, or by a combination of methods. In the analytical case, it is useful to subdivide each panel into a number of smaller elements, applying the methods of conventional finite element analysis to find the stiffness of the assemblage of smaller elements. Determination of panel stiffness will be treated more fully in the following section.

Marginal members at the perimeter of the diaphragm and intermediate purlins are usually made of standard rolled beams or cold formed sections. For the analysis, they are represented as one-dimensional elements, able to resist axial loads as well as bending about their vertical axis. Accordingly, three degrees of freedom are chosen at each end of each

segment: two translational (both in the horizontal plane) and one rotational (about the vertical axis). The corresponding 6 x 6 stiffness matrix for each segment is formed in the standard way and incorporated into the analytical model by direct superposition. Where internal hinges are to be assumed, as at the junction of purlins and marginal beams, bending rigidity is relaxed by modifying the member stiffness at that junction using principles of static condensation (4).

In an actual diaphragm, panels are connected to each other or to marginal members and purlins at discrete locations using welds or sheet metal screws. In the model, dual nodal points are established at such locations, one on each part. These are assumed to be interconnected by a two-dimensional spring, with the axes parallel and perpendicular to the axes of the members joined, as shown in Fig. 5. The effects of the slight movement that occurs between connected parts when load is applied is simulated by these spring linkages. In the model, the dimensions of such linkages are reduced to zero, i.e., the nodal point coordinates are identical for both parts at any connector location.

Spring constants are established by experimental means, using a small test apparatus shown in Fig. 6. The figure shows a welded seam connection clamped between rigid plates and loaded in shear. Deformation in the weld and in the panel steel immediately adjacent to it is measured by the dial gages.

Having the stiffness matrix for each component of a shear diaphragm, the stiffness matrix for the entire assemblage is obtained by superimposing member stiffnesses as for a direct stiffness type of solution (4). Force and displacement boundary conditions are imposed on the resulting set of joint equilibrium equations, and the system is solved for the displacements at the nodal points. After this, element stiffness matrices are used once again, to obtain the nodal point forces acting on the individual panels, the marginal beams and purlins, and the connectors.

The solution of the equilibrium equations for the unknown displacements is not a trivial problem because of the number of unknowns and the size of the stiffness matrix to be inverted. It has been found by comparative studies that for present purposes the direct elimination of unknowns provides the fastest and best solution. A solution algorithm developed by Irons (7) was found to be well suited to the present work.

Only linear elastic behavior is considered in the present work. The linear elastic analysis permits calculation of the effective shear modulus which, in accordance with the AISI diaphragm manual, is to be found at 40 percent of failure load. In addition, the elastic analysis permits, for the first time, a detailed study of the distribution of internal forces acting on the components and connections, and thus represents a major step toward balanced design. A lower bound on the strength can be obtained by assuming elastic behavior up to that load

which produces failure in the most highly stressed part (usually a connector). Actually diaphragms do not behave in this way. Because of local plastic deformation and resulting redistribution of internal forces, they continue to carry higher loads, although local plastic deformations result in non-linear load-deflection response above about 40 percent of failure load. Neglect of this redistribution gives a conservatively low estimate of the actual strength. On the basis of limited comparisons, it appears that such strength estimates are actually rather close to the true value.

Methods for Deriving Panel Stiffness

Of the several element types used in the analysis, the most difficult with respect to formulation of the stiffness matrix is the panel sheet itself. If the panel offers a flat shear surface the modelling is quite simple; the panel sheet can be considered isotropic, in a state of plane stress. The modelling of a panel with open geometry, such as a standard corrugated sheet, is much more difficult because of the geometrically-imposed orthotropy.

Three alternative methods were employed for panels of the second type. The first was experimental and required testing of a single complete panel. The second was analytical and made use of a high order curved finite element to model the panel geometry. The third combined experimental and analytical means, and led to a simulation of the panel as an equivalent

flat orthotropic sheet, with extensional and shear moduli determined by experiment. While the third method was finally adopted, the first and second are not without merit, and will be described briefly.

(a) Panel Stiffness by Inversion of Experimental Flexibility

When experimental methods are used, it is generally easier to obtain the flexibility matrix, after which the desired stiffness matrix can be found by inversion. Accordingly, a test frame was built, as shown in Fig. 7. Statically determinate support linkages were provided and load applied at each nodal point, in each of the two principal directions in turn, by a hydraulic jack. The two components of displacement at all nodal points were recorded for each load case. In this way, for each loading, a normalized vector of nodal displacements was obtained. These were assembled as the individual columns of the panel flexibility matrix F, relating a column vector of nodal forces P_f to the column vector of displacements d_f:

$$\{d_f\} = [F]\{P_f\} \tag{1}$$

The panel stiffness matrix K, relating nodal forces to nodal displacements through the equation

$$\{P\} = [K]\{d\} \tag{2}$$

can be found from the experimental F matrix by inversion with appropriate matrix transformation to account for the reaction forces (2,3).

This procedure was followed to obtain the stiffness matrix of a 2' x 8' standard corrugated panel of 26 gage material. While conceptually attractive, practical difficulties were encountered due to the strong orthotropy of the corrugated panels, as well as the difficulty in reducing frictional restraint. As a result the method was not used for the present work.

(b) Panel Stiffness by Finite Element Analysis

This method consists of a piece-wise modelling of the corrugation geometry, using a high-order cylindrical finite element, as shown in Fig. 8, rectangular in its horizontal projected shape, with 12 degrees of freedom at each of its 4 nodes: u, v, and w displacements, their first derivatives with respect to x and y, and the mixed second derivatives with respect to x and y. An array of such elements, alternately concave up and concave down, were used to represent a corrugated panel. Displacement boundary conditions and loading were imposed to correspond with the conditions produced in the experimental determination of flexibility. Reasonably good agreement with tests was obtained where reliable test figures were available (off-diagonal flexibility terms from the tests being questionable). The great disadvantage of the method is that a very large number of degrees of freedom are needed for the finite element solution (800 degrees of freedom for a 2' x 2' panel, for example). Because of this, the method was not pursued further.

(c) Panel Stiffness Using an Equivalent Flat Orthotropic Plate

The method finally adopted was based on a modelling of the corrugated sheet using an equivalent orthotropic thin plate of uniform thickness. A rectangular element was used, with two translational degrees of freedom at each corner node, and with an assumed linear displacement function, as shown in Fig. 9. Any given panel was represented as an aggregation of such elements.

In order to develop the 8 x 8 stiffness matrix for the orthogonal plane stress element, the displacement functions were differentiated to obtain element strains such that

$$\{e\} = [D]\{d\} \tag{3}$$

where $\underline{e}$ is the column vector of extensional and shear strains, and d the column vector of nodal displacements. Next the constitutive relations were introduced relating stresses s to strains e:

$$\{s\} = [E]\{e\} \tag{4}$$

where for the specially orthogonal element:

$$E = \frac{1}{1 - \nu_{xy}\nu_{yx}} \begin{bmatrix} E_{xx} & \nu_{yx}E_{xx} & 0 \\ \nu_{xy}E_{yy} & E_{yy} & 0 \\ 0 & 0 & (1-\nu_{xy}\nu_{yx})G_{xy} \end{bmatrix} \tag{5}$$

In this equation, E_{xx} and E_{yy} are the extensional moduli in the X and Y directions, respectively, G_{xy} is the shear modulus,

ν_{yx} is the Poisson's ratio relating induced strain in the X direction to imposed strain in the Y direction, and ν_{xy} relates induced strain in the Y direction to imposed strain in the X direction.

Then, by application of the principle of stationary potential energy (13), the relation between nodal forces P_i and nodal displacements d_i can be found:

$$P_i = \left[\int_{vol} [D]^T [E] [D] dv \right] d_i \qquad (6)$$

where the quantity in square brackets represents an 8 x 8 array of coefficients, by definition equal to the stiffness matrix for the orthotropic element. The specific entries in the element K matrix can be found in Ref. 3 .

The elastic constants of Eq. (5) must be derived considering not only the properties of the base material, but the geometry of the cross section as well. The basis of the equivalent orthotropic element may be clarified by reference to Fig. 10 which shows a section of corrugated plate of length a, width b, developed width ℓ, and thickness t as well as an equivalent plate of the same projected dimensions and same thickness. A load P in the longitudinal direction produces a stress $P/\ell t$ in the corrugated plate and a stress P/bt in the equivalent plate. The deflection Δ is to be equal in the two cases. It is easily shown that the extensional modulus E_{yy} for the equivalent plate is equal to

$$E_{yy} = E_o(\ell/b) \qquad (7)$$

The other terms of Eq. (5) are defined in a similar sense. The transverse modulus E_{xx} and the shear modulus G_{xy} are most easily found experimentally.

Diaphragm Simulation and Correlation with Experimental Results

The analysis was applied to simulate the behavior of several diaphragms for which experimental data were available, to predict the effective shear rigidity. In addition, the analysis provides much information regarding the internal distribution of forces. Most of this data has no experimental counterpart, because to obtain it would have required excessive instrumentation, and because of the highly indeterminate nature of diaphragms, which prevents the separation of effects, e.g., the division of shear force along a seam between seam and end welds.

The diaphragms studied were of two types. The first panels had a continuous flat sheet stiffened by hat sections, while the second used panels having a single corrugated surface. Because of space limitations, only one test, of the first type, will be described here.

The prototype diaphragm was tested at Cornell as a part of an extended series for Fenestra, Inc. (12), and is shown in Fig. 4 and Fig. 11. The test was conducted using a horizontal shear frame measuring 10' x 12' and bounded by 10" and 12" marginal wide flange beams. No purlins were used. Statically determinate external supports were provided: a hinge at the

southeast corner and a roller at the northeast. The rectangular area bounded by the marginal beams was decked using standard double hat section panels, 2' wide and 10' long. Both the 24" wide flat sheet and the hat sections were of 16 gage material. Load was applied by a hydraulic jack at the southwest corner of the diaphragm, and displacements measured by dial gages at key locations indicated by the letters A through I.

The analytical model is shown in Fig. 12. The north and south marginal beams are modeled into 5 linear segments, each 2' long. For each segment 3 degrees of freedom are established at each end: longitudinal, transverse, and rotational. The west and east marginal beams are modeled in a similar fashion, using 6 subassemblies, each consisting of 2 beam segments.

Each deck panel is idealized into 5 subassemblies 2' square, each composed of 8 isotropic finite elements. The extensional moduli E_{xx} and E_{yy} were taken equal to 30,000 ksi, Poisson's ratios in each direction equal to 0.3, and the shear modulus G_{xy} 11,500 ksi.

The panel-to-beam edge welds, 4 in number on each side, are represented by springs having stiffness of 800 kips per inch, based on separate tests. Panel end welds were similarly represented, the spring constant being 1000 kips per inch.

Seam welds were represented in the same manner. Based on tests, the stiffness in the longitudinal direction was 500 kips per inch, while in the transverse direction an arbitrarily high value of 10,000 kips per inch was used.

The predictions of the elastic analysis may be compared with experimental results at about 50 percent of failure load (jack load of 20 kips). Up to this load, the performance of the actual diaphragm was essentially elastic. Direct comparison is possible of the values for deflection at the jack, and for seam slip at gages G, H, and I (see Fig. 11):

	Deflection at jack (in.)	Seam slip (in.)		
		Gage G	Gage H	Gage I
Computed values	0.0656	0.0063	0.0062	0.0063
Test values	0.0660	0.0080	0.0080	0.0080

It is seen that the test values of seam slip are underestimated by about 20 percent. This may be due to differences in technique in making the welds for the connection tests (on which the analytical spring stiffness was based) and in making those for the actual diaphragm test which was done some years earlier. The deflection at the jack, which provides the basis for the calculation of effective shear modulus, is confirmed within less than 1 percent.

In addition to these results, which are compared with experimental values, extensive information is available from the analysis regarding the distribution of forces in the diaphragm.

Fig. 13 shows the variation of lateral forces imposed on the marginal beams from the panel end and edge welds. A tensile force between beam and panel is defined as positive. At

the panel ends (forces on east and west beams) a typical pattern of forces is disclosed in which compression is present at one panel corner and tension at the other corner of the same panel end. The lateral force transferred at the center weld of each group of three welds is very small. At adjacent panel corners, forces are of opposite sign and nearly cancel, confirming that, in general, the panel end welds serve the same function as the seam welds in preventing seam slip between panels; however, at the ends the shear force is transmitted from panel to beam to panel, rather than directly between panels. The important exception to this force pattern is at the corners of the decked area, where the perimeter shear is transferred to the diaphragm. Note that the lateral force at the north end of the east beam is identically the same as the longitudinal force at the east end of the north beam, as plotted in Fig. 14. Lateral forces imposed on the marginal beams running parallel to the panel span are very small.

The longitudinal forces transferred at each weld between marginal beam and adjacent panel are shown in Fig. 14. It is clear that the transmittal of shear into the diaphragm along the west beam, and out of the diaphragm along the east beam, is more or less uniform. Longitudinal forces along the north and south beams, which run parallel to the panel span, show some variation along the length.

The shear transfer at the seam welds is shown in Fig. 15. Seam no. 1 is 2' from the north edge of the diaphragm, seam

no. 2 is at the center, and seam no. 3 is 2' from the south edge. In contrast with the usual assumption of uniform transfer of shear force along a typical seam, a distinct parabolic variation is obtained.

A strength estimate was made on the basis of the elastic analysis, neglecting redistribution of internal forces due to local plasticity. Inspection of the computer output corresponding to a jack load of 20 kips revealed that the puddle weld in the southeast corner of the deck was stressed to the largest fraction of its strength. At 20 kips, the force components on that connector, in the directions parallel and perpendicular to the panel axis, respectively, were 2.885 kips and 1.818 kips. Accordingly the resultant force is

$$F = \sqrt{(2.885)^2 + (1.818)^2} = 3.42 \text{ kips}$$

On the basis of tests of 1" diameter puddle welds with 16 gage material it is known that the strength is 6.3 kips. Accordingly the strength prediction, based on elastic behavior, is

$$P_u = 20.0 \times (6.3/3.42) = 36.8 \text{ kips}$$

This represents 95 percent of the experimentally determined value of $P_u = 38.6$ kips.

The computer time needed for the solution, which in this case involved a system containing 900 unknowns, included 10 seconds for generation of the data, 65 seconds of processing time, 65 seconds for input and output. This total of 140

seconds should be considered as the "net time" of execution, the program having been precompiled, edited, and stored on disk. If this were not the case, an additional 90 seconds is required for compilation and editing.

Summary and Conclusions

A method of analysis has been presented for shear diaphragms composed of light gage steel panels, marginal beams, and purlins. Plane stress finite elements are used to model the panels, line elements to model the purlins and marginal members, and specially-devised linkage elements to represent the connectors between panels, as well as the connectors joining panels and frame members. The mechanical properties of each type of component are found separately, by analysis or test, and the components assembled analytically using a direct stiffness matrix approach. The elastic analysis of the resulting assemblage provides an alternative to full-scale shear diaphragm testing to determine the effective shear modulus. It also permits a conservative estimate of shear strength.

A number of diaphragms have been analyzed and the results compared with existing experimental data. Because of space limitations, only one such case is reported here. In general, agreement between analysis and experiment has been excellent. The single exception has proved to be for longer span diaphragms of the type using open, corrugated panels, for which experimental deflections were significantly less than those predicted

by analysis. While the error is on the safe side, it appears desirable to investigate further the effect of span length when dealing with panels of this type.

It is desirable also to extend the analysis into the inelastic range. It is known from many tests that the limit of elastic response for typical diaphragms is about 40 percent of the failure load. The main source of non-linearity is the connectors. The present analysis could be used as the basis for studies in the inelastic range by adopting an incremental loading scheme, combined with iteration at each load increment to converge on correct stiffnesses at that increment for each connector. While limited comparisons have indicated that strengths predicted on the basis of elastic analysis are within about 10 percent of the true experimental strengths, plasticity effects must be included if this figure is to be improved.

In addition to providing the value of effective shear modulus, and establishing a lower limit of strength, the present analysis provides much information about the magnitude and distribution of forces in shear diaphragms. For the first time, the transfer of shear force along seams can be studied, the sharing of shear load between seam fasteners and panel end connections established, and the distribution of longitudinal and transverse forces on marginal beams and purlins found. By studying such results, and noting the effect of changes in the important parameters, it should be possible to optimize the design of diaphragm systems.

Acknowledgements

The experimental and analytical work on which this paper is based was carried out by Albert R. Ammar, research assistant at Cornell University, working under the direction of the author. Dr. Craig Miller, formerly research assistant at Cornell, contributed significantly in the development of the computer program. The work was funded by the American Iron and Steel Institute through research grant no. 1201-201 to Cornell University.

References

(1) "Design of Light Gage Steel Diaphragms", Amer. Iron and Steel Inst., New York, 1967.

(2) Ammar A. R. and Nilson A. H., "Analysis of Light Gage Steel Shear Diaphragms - Part I", Research Report No. 350, Dept. of Structural Engg., Cornell Univ., Aug. 1972.

(3) Ammar A. R. and Nilson A. H., "Analysis of Light Gage Steel Shear Diaphragms - Part II", Research Report No. 351, Dept. of Structural Engg., Cornell Univ., Apr. 1973.

(4) Beaufait F. W., Rowan W. H., Hoadley P. G., and Hackett R. M., "Computer Methods of Structural Analysis", Prentice-Hall Inc., New Jersey, 1970.

(5) Bryan E. R. and El-Dakhakhni W. M., "Behaviour of Sheeted Portal Frame Sheds: Theory and Experiments", Proc. Inst. of Civil Engineers, Vol. 29, Dec. 1964.

(6) Bryan E. R. and El-Dakhakhni W. M., "Shear Flexibility and Strength of Corrugated Decks", Journal of Struct. Div., ASCE, Vol. 94 No. ST11, Nov. 1968.

(7) Irons B. M., "A Frontal Solutions Program for Finite Element Analysis", Int. Journ. for Numerical Methods in Engg., Vol. 2 No. 1, Jan.-Mar. 1970.

(8) Luttrell L. D., "Structural Performance of Light Gage Steel Diaphragms", Research Report No. 319, Dept. of Structural Engg., Cornell Univ., Aug. 1965.

(9) Miller C. J., "Analysis of Multistory Frames with Light Gage Steel Panel Infills", Research Report No. 349, Dept. of Structural Engg., Cornell Univ., Aug. 1972.

(10) Nilson A. H., "Shear Diaphragms of Light Gage Steel", Journ. of Structural Div., ASCE, Vol. 86 No. ST11, Nov. 1960.

(11) Nilson A. H., "Folded Plate Structures of Light Gage Steel", Journal of Structural Division, ASCE, Vol. 87 No. ST7, Oct. 1961.

(12) Nilson A. H., "Report on Tests of Light Gage Steel Floor Diaphragms - 1957 Series", Research Report, Dept. of Structural Engg., Cornell Univ., 1957.

(13) Zienkiewicz O. C. and Cheung Y. K., "The Finite Element Method in Structural and Continuum Mechanics", McGraw-Hill Ltd., London, 1967.

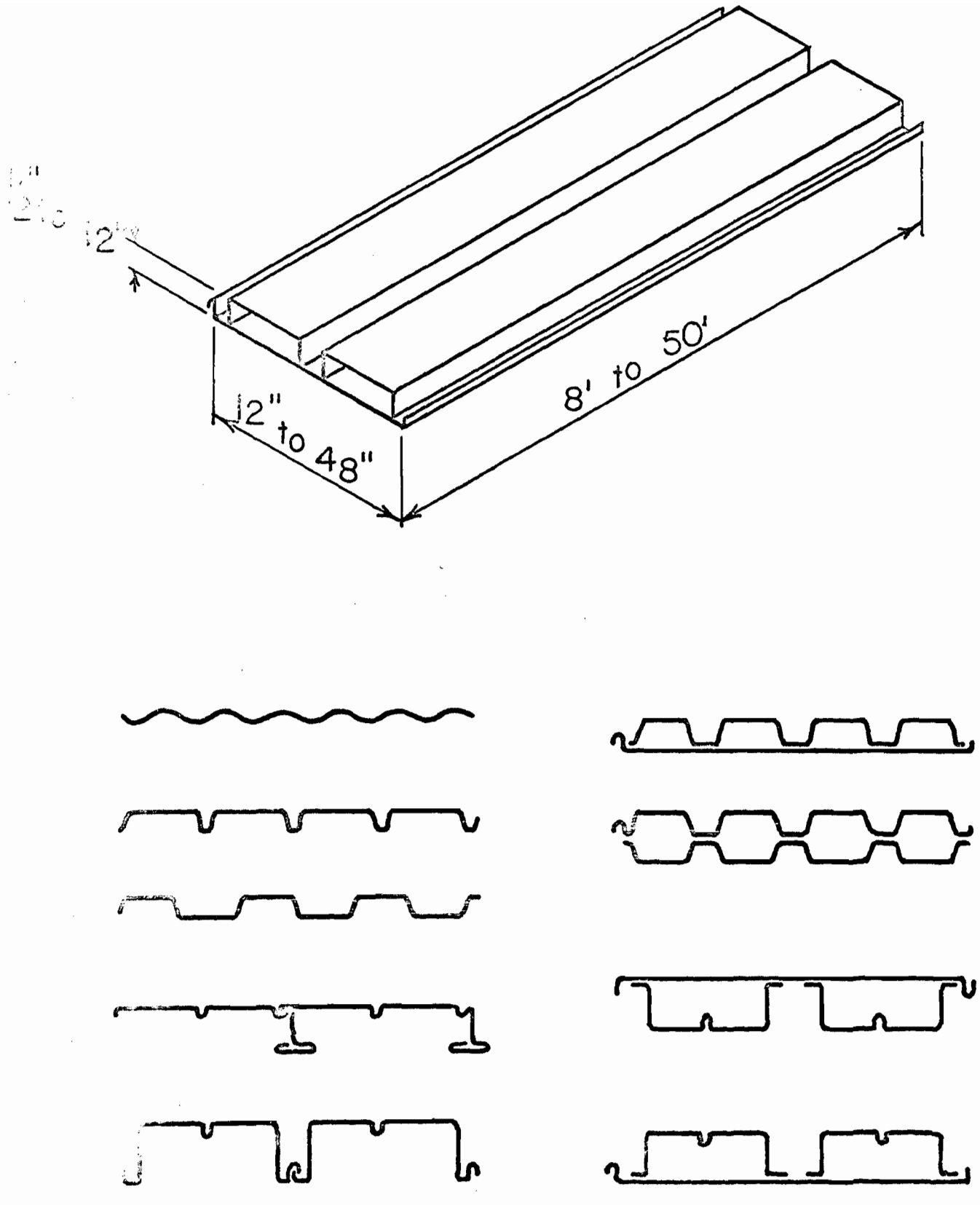

Fig. 1 Types of light gage steel panels

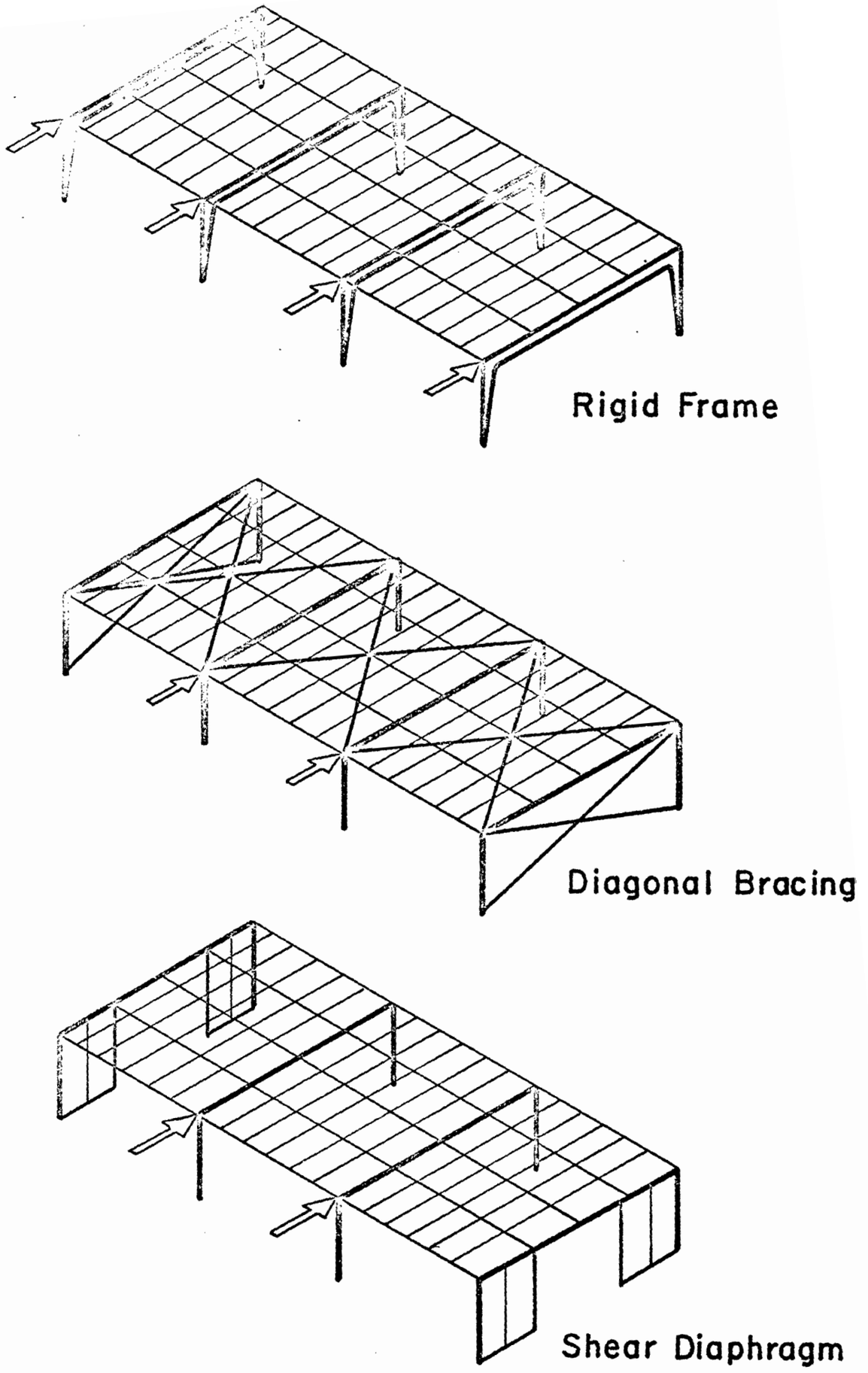

Fig. 2 Alternative methods for resisting lateral forces

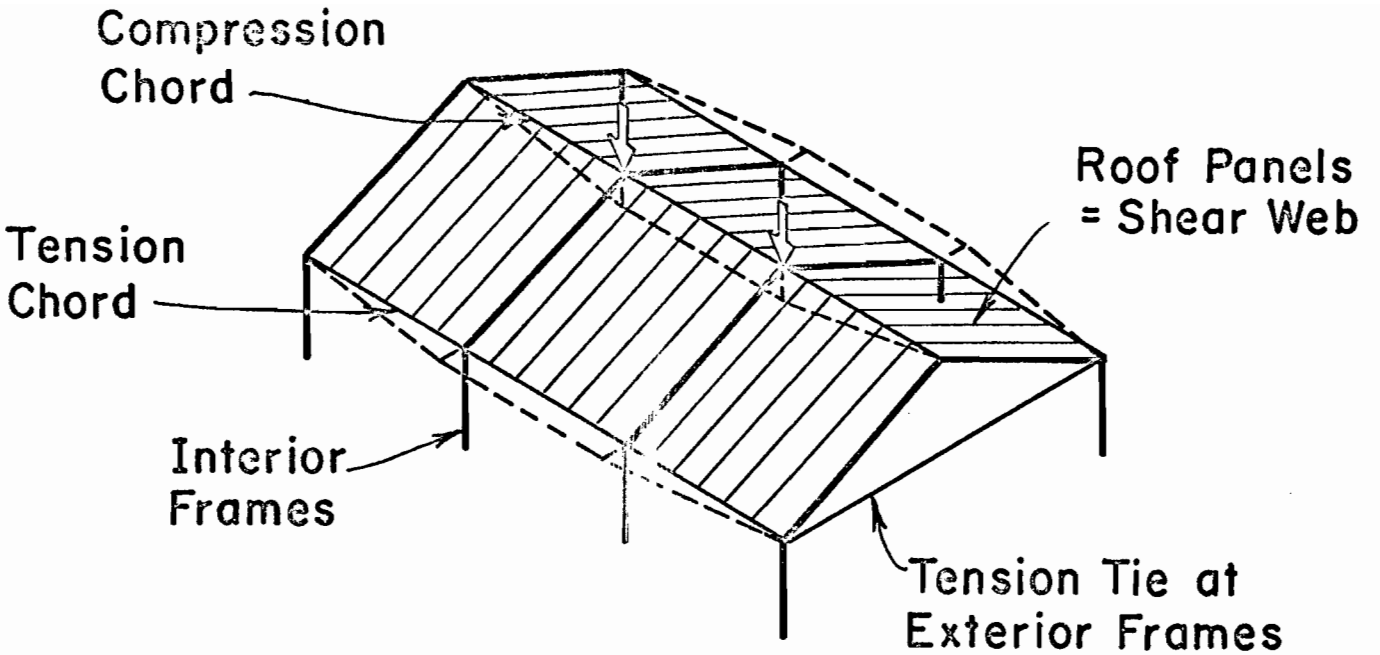

Frame Cladding Interaction

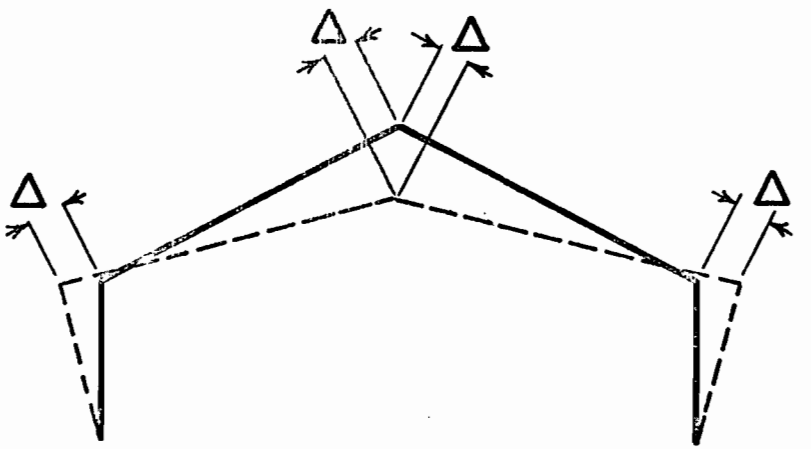

Cross Section at Interior Frames

Fig. 3 Interaction of sheathing and moment resisting frames to

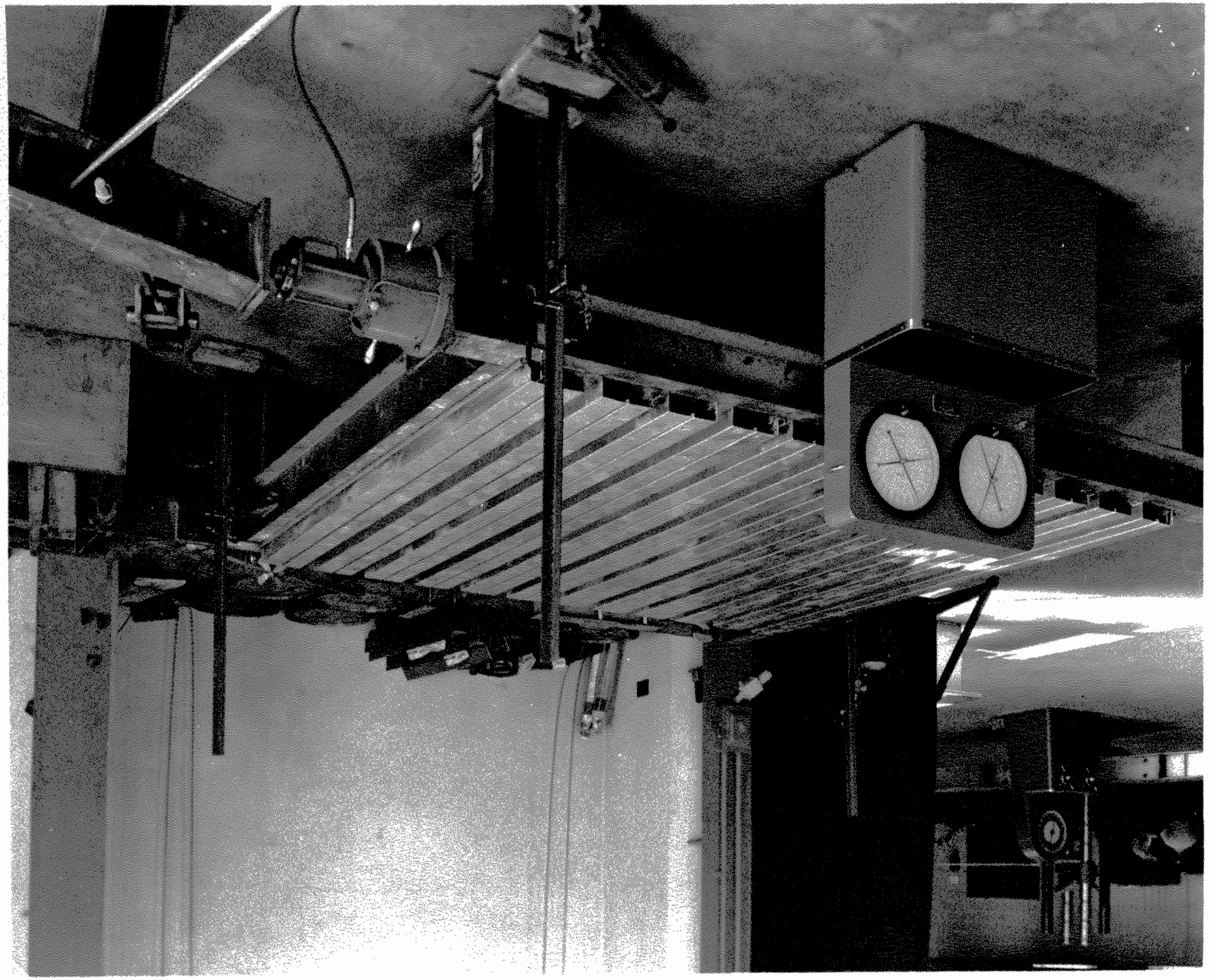

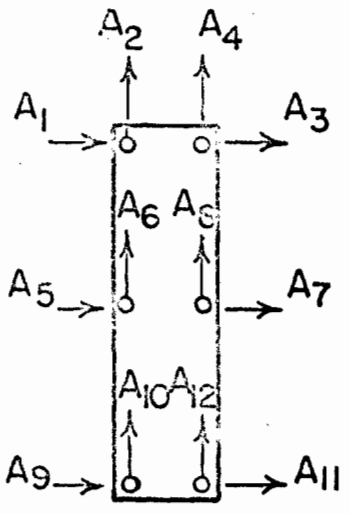

$$\begin{bmatrix} A_1 \\ A_2 \\ A_3 \\ A_4 \\ A_5 \\ A_6 \\ A_7 \\ A_8 \\ A_9 \\ A_{10} \\ A_{11} \\ A_{12} \end{bmatrix} = \begin{bmatrix} & & \\ & K_p & \\ & & \end{bmatrix} \begin{bmatrix} d_1 \\ d_2 \\ d_3 \\ d_4 \\ d_5 \\ d_6 \\ d_7 \\ d_8 \\ d_9 \\ d_{10} \\ d_{11} \\ d_{12} \end{bmatrix}$$

Panels

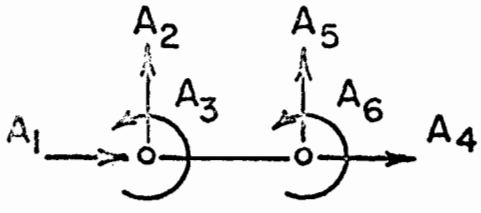

$$\begin{bmatrix} A_1 \\ A_2 \\ A_3 \\ A_4 \\ A_5 \\ A_6 \end{bmatrix} = \begin{bmatrix} & & \\ & K_b & \\ & & \end{bmatrix} \begin{bmatrix} d_1 \\ d_2 \\ d_3 \\ d_4 \\ d_5 \\ d_6 \end{bmatrix}$$

Beams

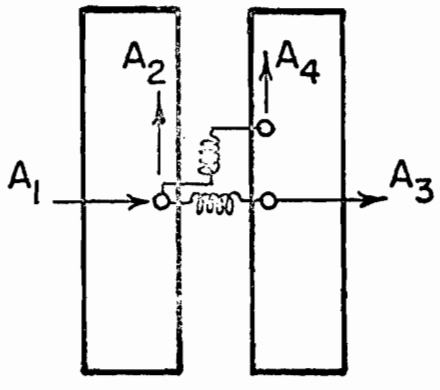

$$\begin{bmatrix} A_1 \\ A_2 \\ A_3 \\ A_4 \end{bmatrix} = \begin{bmatrix} & & \\ & K_s & \\ & & \end{bmatrix} \begin{bmatrix} d_1 \\ d_2 \\ d_3 \\ d_4 \end{bmatrix}$$

Connectors

Fig. 5 Types of elements used in the analysis and corresponding stiffness matrices

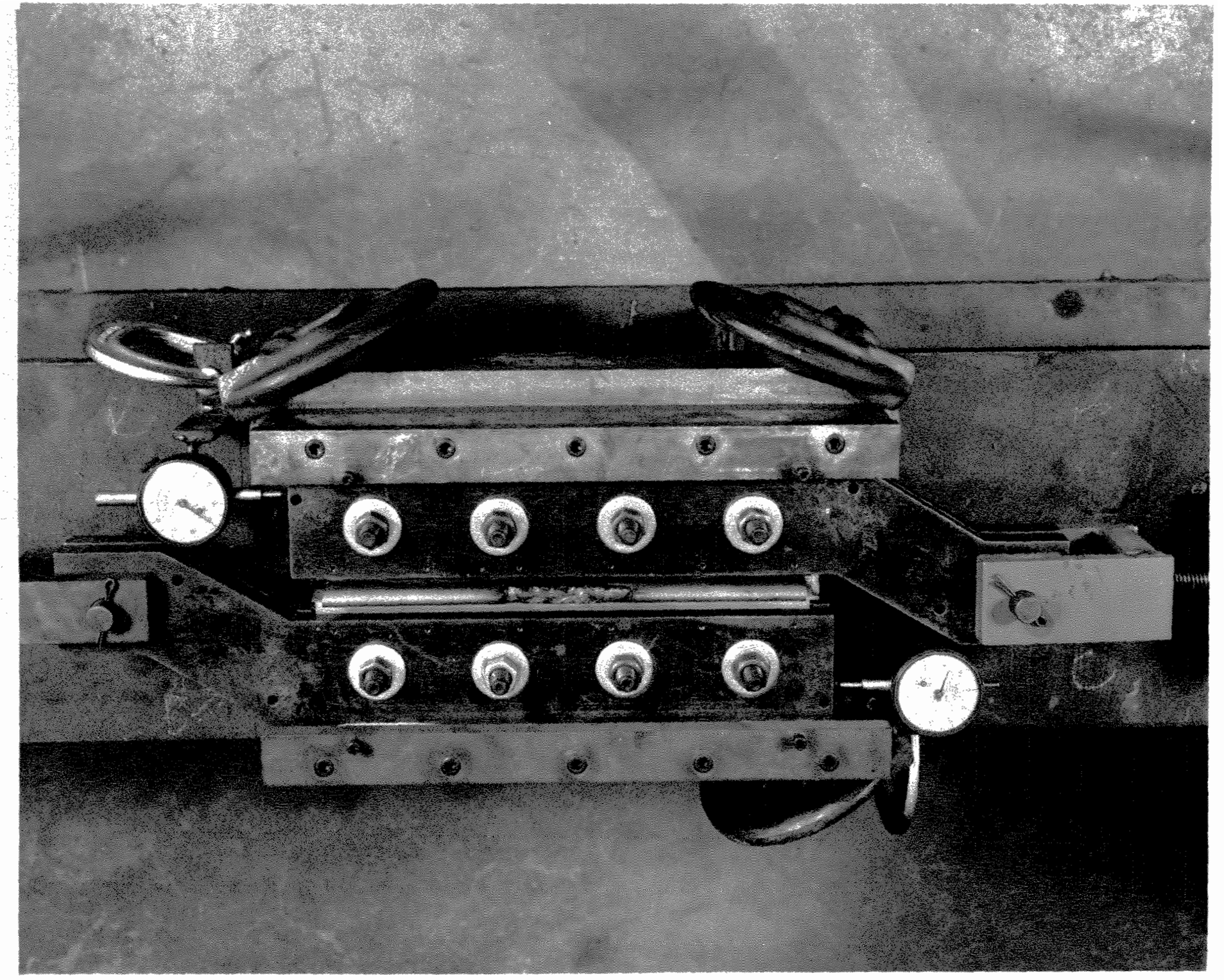

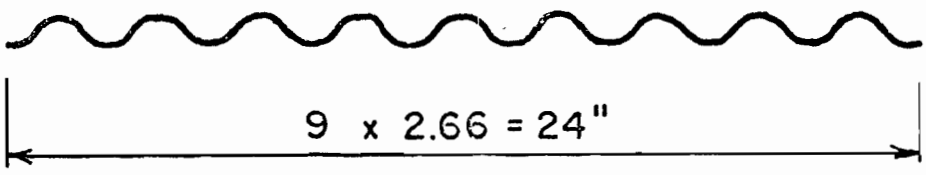

a) Corrugated sheet

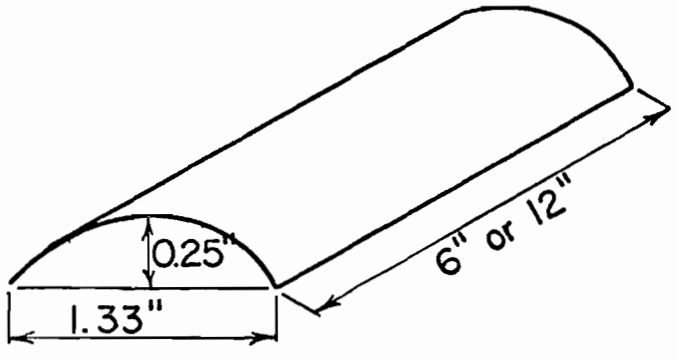

b) Curved finite element

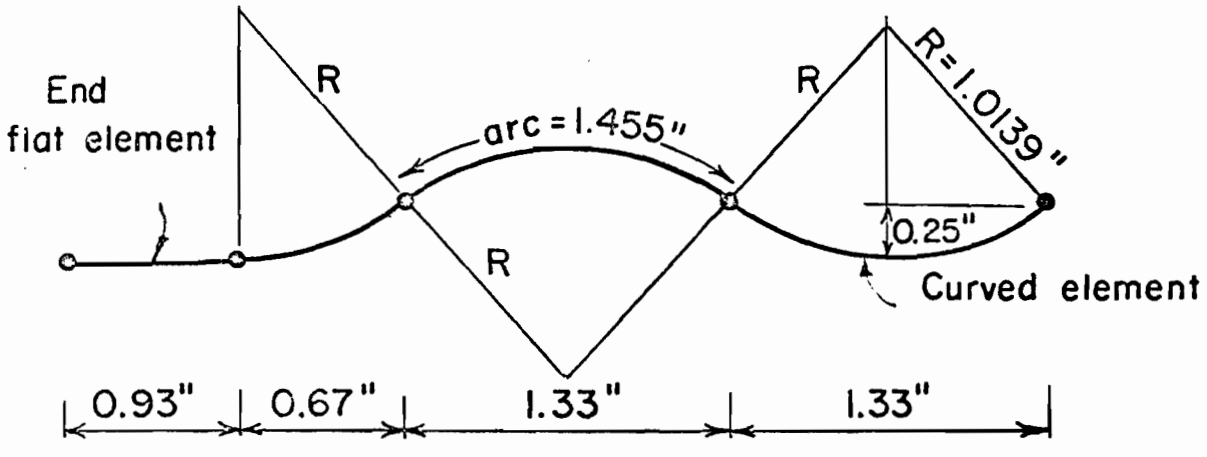

c) Assemblage of curved finite elements

Fig. 8 Modeling of corrugated sheet using cylindrical finite element with 48 degrees of freedom

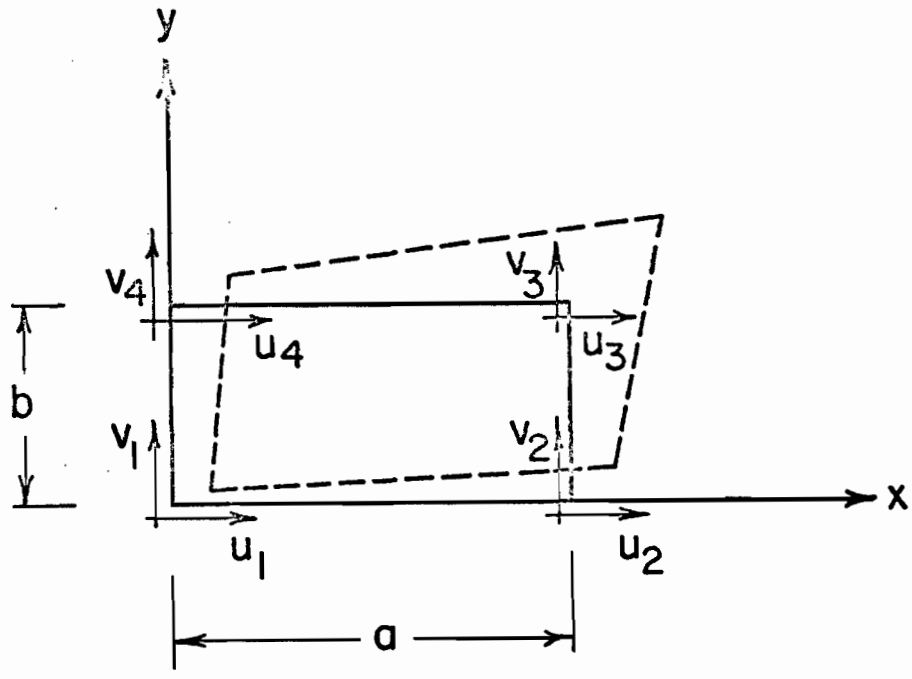

$$u = \left[\left(1-\frac{y}{b}\right)\left(1-\frac{x}{a}\right)\right]u_1 + \left[\left(1-\frac{y}{b}\right)\frac{x}{a}\right]u_2 + \left[\frac{y}{b}\ \frac{x}{a}\right]u_3 + \left[\frac{y}{b}\left(1-\frac{x}{a}\right)\right]u_4$$

$$v = \left[\left(1-\frac{y}{b}\right)\left(1-\frac{x}{a}\right)\right]v_1 + \left[\left(1-\frac{y}{b}\right)\frac{x}{a}\right]v_2 + \left[\frac{y}{b}\ \frac{x}{a}\right]v_3 + \left[\frac{y}{b}\left(1-\frac{x}{a}\right)\right]v_4$$

Fig. 9 Orthotropic rectangular finite element and assumed displacement function

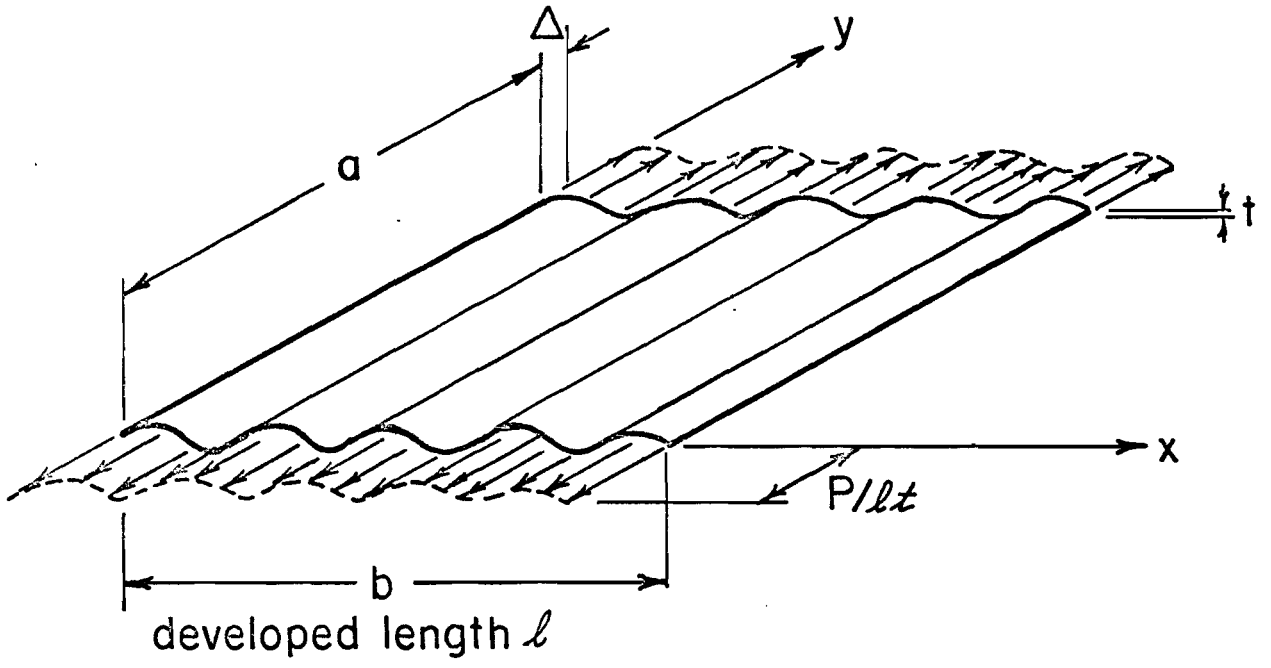

Corrugated panel

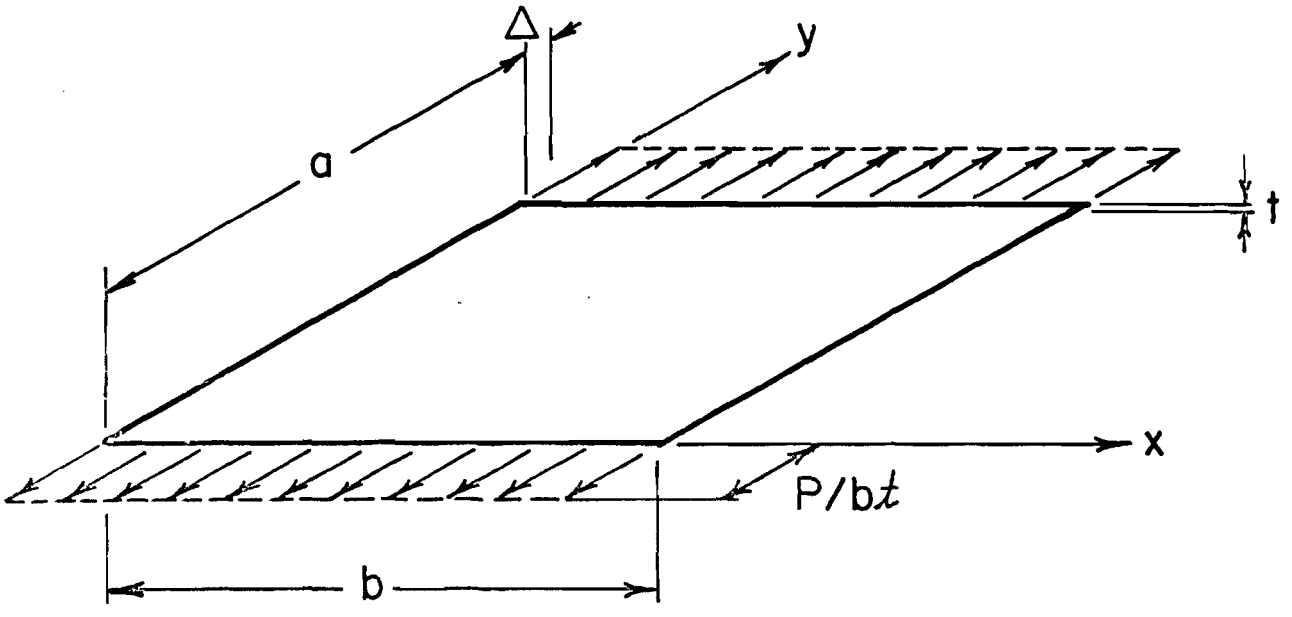

Equivalent orthotropic plate

Fig. 10 Basis of equivalent orthotropic element

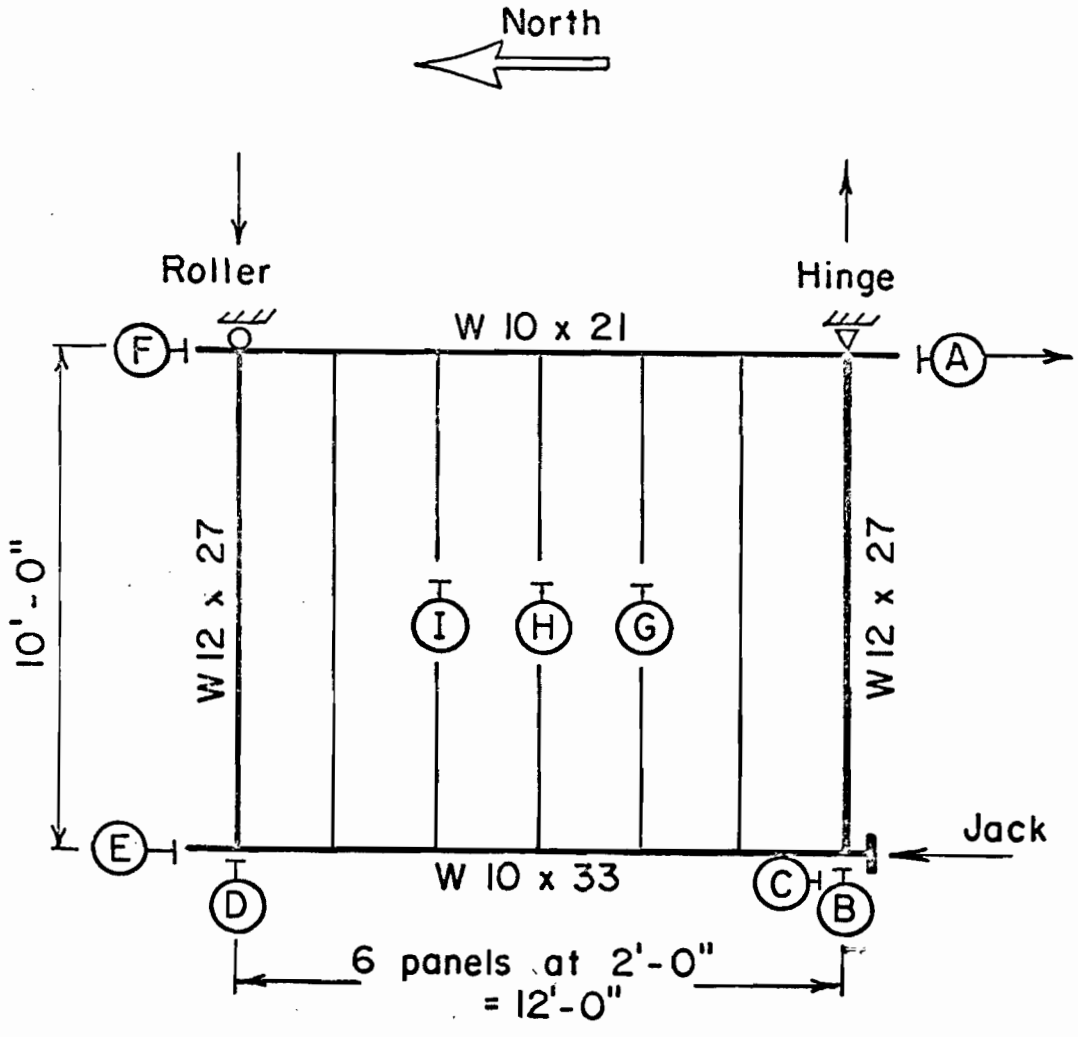

Fig. 11 Test arrangement for 6 panel diaphragm

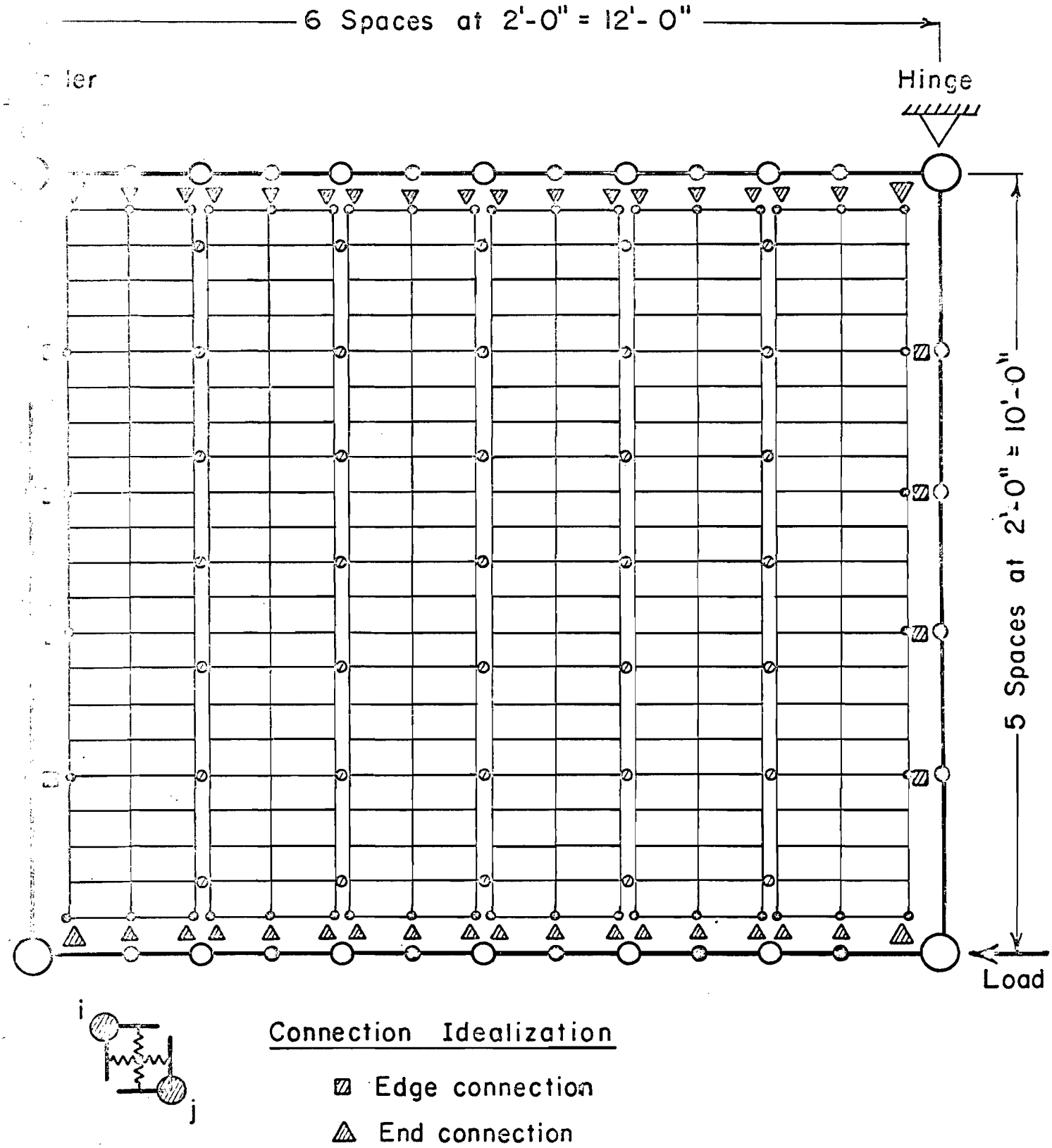

Fig. 12 Analytical representation of diaphragm

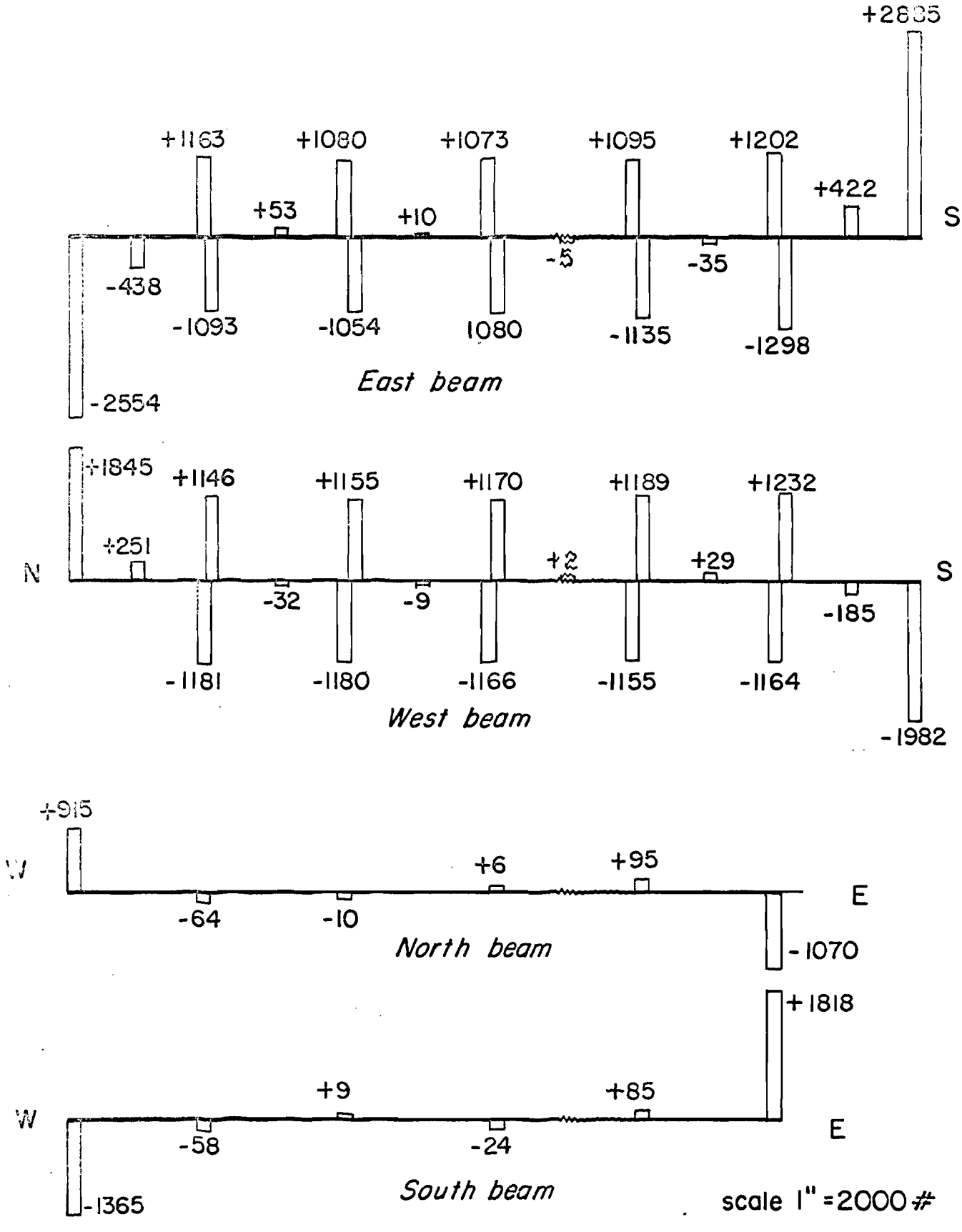

Fig. 13 Lateral forces on marginal members from analysis

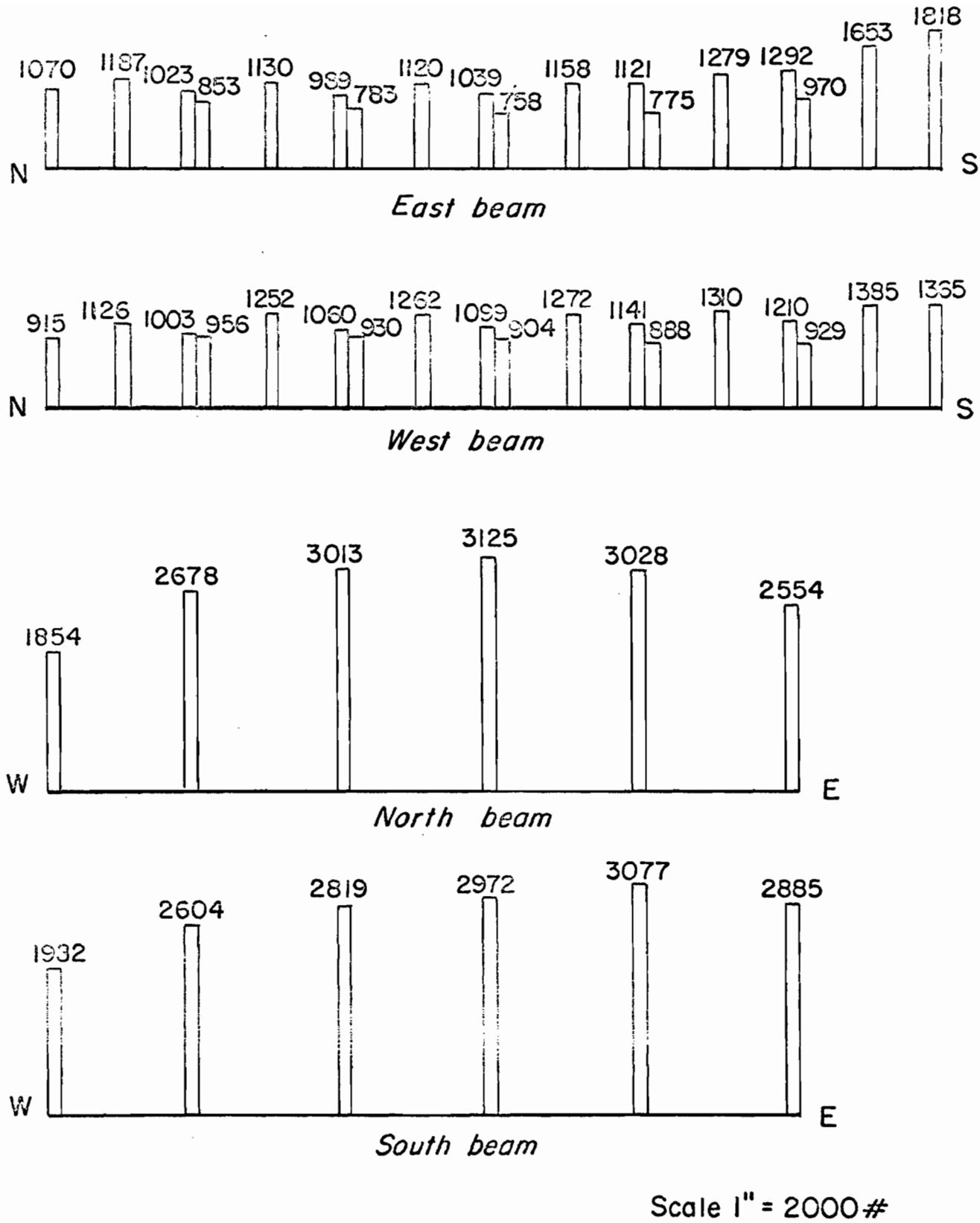

Fig. 14 Longitudinal forces on marginal members from analysis

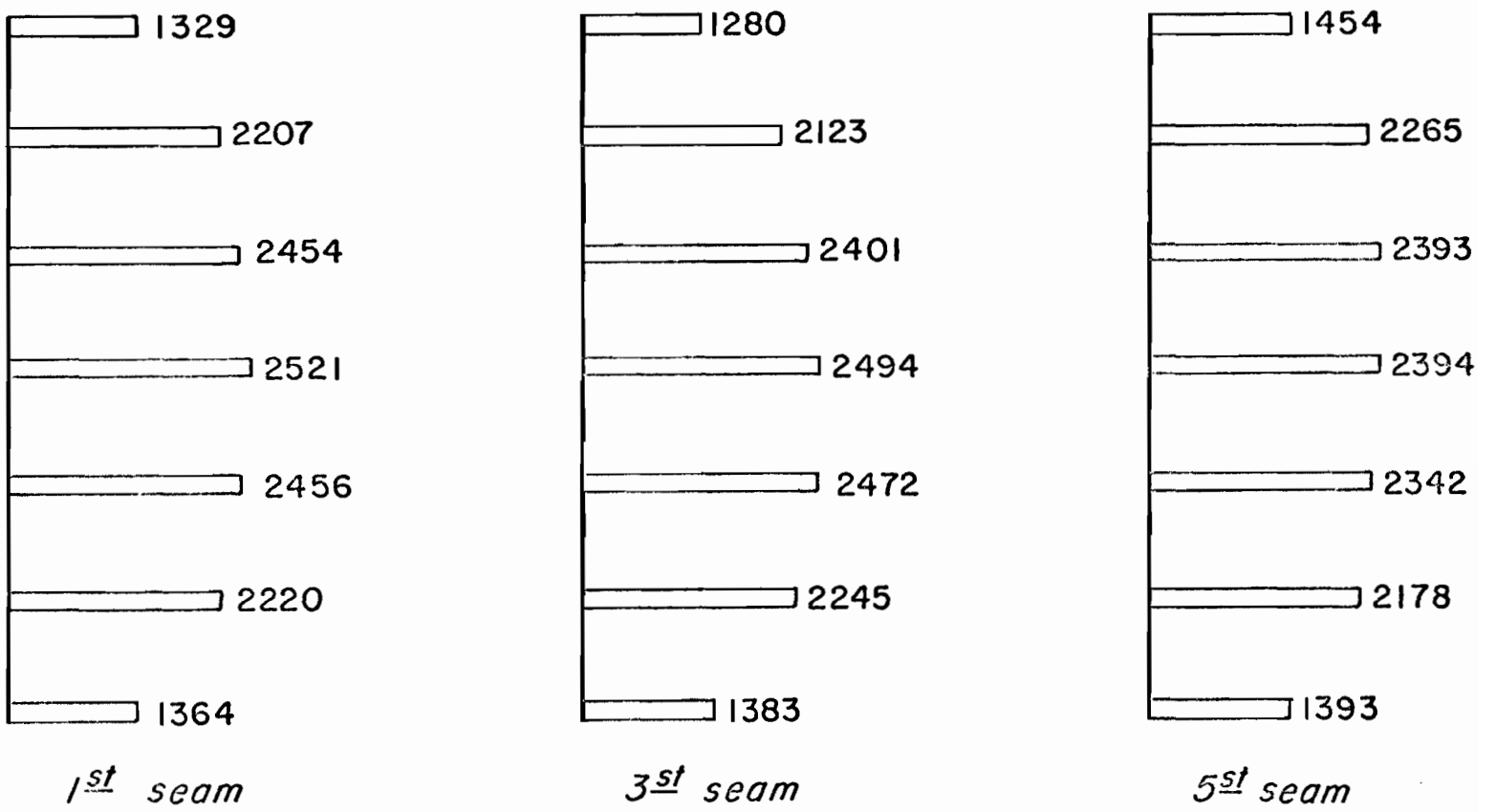

Fig. 15 Distribution of longitudinal forces at seam connectors